Sequential Ordered Fatty Acid α Oxidation and Δ9 Desaturation Are Major Determinants of Lipid Storage and Utilization in Differentiating Adipocytes†

Xiong Su,‡ Xianlin Han,§ Jingyue Yang,‡ David J. Mancuso,§ Jeannie Chen,|| Perry E. Bickel,||,⊥ and Richard W. Gross*,‡,§,@

Division of Bioorganic Chemistry and Molecular Pharmacology, Department of Internal Medicine, Division of Endocrinology, Metabolism, and Lipid Research, Department of Internal Medicine, and Departments of Chemistry, Molecular Biology and Pharmacology, and Cell Biology and Physiology, Washington University School of Medicine, St. Louis, Missouri 63110

Received October 16, 2003; Revised Manuscript Received January 22, 2004

ABSTRACT: Herein, we exploit the power of global lipidomics to identify the critical role of peroxisomal processing of fatty acids in adipocyte lipid storage and metabolism. Remarkably, 3T3-L1 differentiating adipocytes rapidly acquired the ability to α oxidize unbranched fatty acids, which is manifested in the accumulation of odd chain length unbranched fatty acids in all major lipid classes. Moreover, in differentiating adipocytes, unsaturated odd chain length fatty acids in TAG molecular species contained exclusively Δ9 olefinic linkages. Unsaturated fatty acids (e.g., oleic and palmitoleic acids) were not subject to α oxidation, resulting in the absence of Δ8 unsaturated odd chain length fatty acids. This highly selective substrate utilization resulted in the obligatory sequential ordering of α oxidation prior to Δ9 desaturation. On the basis of these results, a putative type 2 peroxisomal localization sequence was identified at the N-terminus of mouse stearoyl-CoA desaturase I (SCD I) comprised of ^{30}**KV**KTVPL**HL**^{38}. Kinetic analysis demonstrated that the rate of α oxidation of exogenously administered [9,10-^{3}H]palmitic acid increased 4-fold during differentiation. Similarly, quantitative PCR demonstrated a 4-fold increase in phytanoyl-CoA α hydroxylase (PAHX) and fatty acyl-CoA oxidase (FACO) mRNA levels during differentiation. Collectively, these results underscore the role of peroxisomal fatty acid processing as an important determinant of the metabolic fate of fatty acids in the differentiating adipocyte.

Understanding the mechanisms underlying chemical energy storage and utilization in adipocytes is central to containing the epidemic of obesity currently afflicting industrialized nations (*1*−*4*). Adipocytes transport fatty acids across their plasma membranes where the carboxylic acid group is activated by ATP-dependent thioesterification. Activated fatty acids can subsequently be incorporated into lipid storage pools (e.g., TAG)[1] or alternatively be utilized as substrates for oxidative catabolism, resulting in the production of heat and chemical energy (e.g., ATP). The relative amount of thermal and chemical energy produced in cells is tightly regulated by modulation of the coupling efficiency of fatty acid oxidation with ATP and heat production (*5*, *6*). In general, in mitochondria, fatty acid oxidation is usually tightly coupled to ATP synthesis, while in peroxisomes, fatty acid oxidation is loosely coupled, generating heat at the expense of chemical energy. In mitochondria, this ratio is modulated by uncoupling proteins and intramitochondrial nonesterified fatty acids (*5*, *6*). However, the mechanisms which modulate the coupling of thermal and chemical energy in peroxisomes are unknown.

To identify the principle metabolic pathways regulating fatty acid flux in differentiating adipocytes, alterations in the lipidome of 3T3-L1 cells during their hormone-induced differentiation into adipocytes were determined by electrospray ionization mass spectrometry (ESI-MS). This model of adipocyte differentiation recapitulates the biochemical, molecular biologic, and ultrastructural characteristics of differentiated adipocytes in mammals, including dramatic increases in intracellular TAG content, augmented transcription and translation of adipocyte specific genes, and the morphologic appearance of adipocytes (*7*−*10*). Moreover, compelling studies have demonstrated that this cell lineage can differentiate into adipocyte tissue that cannot be distinguished from existing adipocytes when grafted into athymic mice (*11*).

Since *de novo* synthesis results in, and dietary sources contain, almost exclusively even chain length fatty acids, the overwhelming majority of lipids in mammalian cells are

† This research was supported from NIH Grants 2PO1HL57278-07, 2RO1HL41250-10, and RO1DK59577.

* To whom correspondence should be addressed: Washington University School of Medicine, Division of Bioorganic Chemistry and Molecular Pharmacology, 660 S. Euclid Ave., Campus Box 8020, St. Louis, MO 63110. Telephone: (314) 362-2690. Fax: (314) 362-1402. E-mail: rgross@pcg.wustl.edu.

‡ Department of Chemistry.

§ Division of Bioorganic Chemistry and Molecular Pharmacology, Department of Internal Medicine.

|| Division of Endocrinology, Metabolism, and Lipid Research, Department of Internal Medicine.

⊥ Department of Cell Biology and Physiology.

@ Department of Molecular Biology and Pharmacology.

[1] Abbreviations: ESI-MS, electrospray ionization mass spectrometry; GC−EI-MS, gas chromatography and electron impact mass spectrometry; PC, phosphatidylcholine; PS, phosphatidylserine; PI, phosphatidylinositol; PE, phosphatidylethanolamine; PG, phosphatidylglycerol; TAG, triacylglycerol; FFA, free fatty acid; C*m*:*n*, fatty acid with *m* carbons and *n* double bonds; PTS 2, peroxisome targeting signal 2; DMDS, dimethyl disulfide; SCD, stearoyl-CoA desaturase; SCP 2, sterol carrier protein 2; PAHX, phytanoyl-CoA α hydroxylase; FACO, fatty acyl-CoA oxidase; PA, phosphatidic acid.

10.1021/bi035867z CCC: $27.50
Published on Web 04/07/2004

comprised of even-numbered fatty acyl moieties. Some branched chain fatty acids (e.g., phytanic acid) must be α oxidized to produce the corresponding fatty acid with one fewer carbon atom to render the resulting branched chain backbone suitable for degradation by β oxidation. The first committed step in phytanic acid α oxidation is its 2-hydroxylation catalyzed by phytanoyl-CoA α hydroxylase followed by sequential oxidation and decarboxylation (*12*, *13*). Prior studies have emphasized the exclusive role of this pathway in the metabolism of branched chain fatty acids since purified mammalian phytanoyl-CoA α hydroxylase failed to α oxidize unbranched long chain fatty acids (*14*). Accordingly, it was not believed that substantial α oxidation of unbranched long chain fatty acids occurred in mammalian cells. However, Mukherji *et al.* (*15*) recently demonstrated that purified peroxisomal phytanoyl-CoA α hydroxylase could α hydroxylate unbranched long chain fatty acids in a test tube if sterol carrier protein 2 (SCP 2) was utilized to present the substrate. However, definitive evidence for α hydroxylation of unbranched long chain fatty acids in mammalian cells has not been forthcoming. Accordingly, the presence and amount of α oxidation of unbranched long chain fatty acid catabolism in eukaryotic cells are unknown. Since small fractional differences in the caloric expenditure over each cell's lifetime have substantial effects on the total mass of accumulated lipids, a role for α oxidation as a modulator of adipocyte lipid mass seems possible. Moreover, all of the genes that are necessary for α oxidation of fatty acids are present in the human genome and are localized to the peroxisomal compartment by virtue of either an N-terminal (type 2) or C-terminal (type 1) peroxisomal localization signal (*12*, *13*, *16*−*19*). During the course of our studies on alterations in lipid metabolism in differentiating adipocytes, we identified the unanticipated time-dependent accumulation of odd chain length fatty acyl moieties in multiple phospholipid classes and TAGs. To explore the biochemical mechanisms underlying this phenomenon, we performed a detailed lipid class and molecular species analysis utilizing electrospray ionization mass spectrometry in conjunction with kinetic radiolabeling experiments to gain insight into the biochemical mechanisms underlying the changes in lipid metabolism in the 3T3-L1 differentiating adipocyte. Herein, we report the identification of robust α oxidation of unbranched long chain fatty acids in a mammalian cell line and the obligatory sequential ordered α oxidation of fatty acids prior to their Δ9 desaturation. Collectively, the results demonstrate the importance of proximal peroxisomal fatty acid processing as an important determinant of the metabolic fate of fatty acids in the adipocyte.

EXPERIMENTAL PROCEDURES

Materials. 3T3-L1 cells were obtained from ATCC (Manassas, VA). DMEM and calf serum were purchased from Life Technologies, Inc. (Rockville, MD), while fetal bovine serum was obtained from BioWhittaker, Inc. (Walkersville, MD). Reagents for reverse transcription and quantitative polymerase chain reaction (PCR) were purchased from Applied Biosystems (Foster City, CA). All radiolabeled fatty acids were purchased from American Radiolabeled Chemicals Inc. (St. Louis, MO). Most other chemicals were purchased from Sigma Chemical Co. (St. Louis, MO)

Cell Culture of 3T3-L1 Cells and Differentiation into the Adipocyte Phenotype. 3T3-L1 cells were cultured to confluence in Dulbecco's modified Eagle's medium (DMEM) containing 10% calf serum (CS) by changing the medium every 2 days as previously described (*20*). Two days after cell confluence, differentiation was initiated by adding differentiation medium [0.5 mM methylisobutylxanthine, 0.25 μM dexamethasone, and 1 μg/mL insulin in DMEM containing 10% fetal bovine serum (FBS)]. Two days later, methylisobutylxanthine and dexamethasone were removed, and insulin (1 μg/mL) was maintained for two more days. Thereafter, cells were grown in DMEM containing 10% FBS in the absence of differentiating reagents by replacing the medium every 2 days. At each time point that was examined, cells were washed with PBS, removed from cell culture plates by trypsin, washed with medium, centrifuged, and washed again with PBS before final pelleting. The cell pellets were collected and stored at −70 °C until future use (typically within 1 or 2 weeks).

Lipid Extraction of Differentiated Adipocytes. Lipids were extracted by a modified Bligh−Dyer technique (*21*) utilizing 50 mM LiCl in the aqueous layer in the presence of appropriate internal standards (15:0−15:0 PG, 14:0−14:0 PS, 14:1−14:1 PC, 15:0−15:0 PE, or T17:1 TAG) (*22*−*25*). The internal standards were selected on the basis of their solubility and the lack of any demonstrable endogenous molecular ions in that region which was verified by periodically acquiring mass spectra without internal standards. The lipid extracts were dried under a nitrogen stream, dissolved in chloroform, filtered through 0.2 μm Gelman acrodisc CR PTFE syringe filters, reextracted, and dried under a nitrogen stream. The final lipid residue was resuspended in a 1:1 chloroform/methanol mixture prior to ESI-MS analysis.

Electrospray Ionization Mass Spectrometry of Adipocyte Lipid Classes. ESI mass spectral analysis of lipid molecular species was performed utilizing a Finnigan TSQ Quantum spectrometer (Finnigan MAT, San Jose, CA) equipped with an electrospray ion source as previously described (*22*−*25*). Typically, a 1 min period of signal averaging in the profile mode was employed for each spectrum of the lipid extract. All samples were diluted in a 1:1 methanol/chloroform mixture prior to direct infusion into the ESI source using a syringe pump at a rate of 2 μL/min. Anionic phospholipids, except PS in the diluted chloroform extracts of 3T3-L1 cell pellets, were analyzed by ESI-MS in the negative ion mode and quantified by comparisons of the individual ion peak intensity with internal standard (i.e., 15:0−15:0 PG) after correction for ^{13}C isotope effects. PS was analyzed in the neutral loss scanning mode (87 amu) to enhance the signal-to-noise ratio due to diminutive amounts of PS in differentiating adipocytes. Phosphatidylserines were quantified by comparisons of the individual ion peak intensity with the phosphatidylserine internal standard (i.e., 14:0−14:0 PS). Prior to the analyses of choline and ethanolamine glycerophospholipids in the diluted cell extracts, LiOH in methanol (50 nmol/mg of protein) was added. Choline glycerophospholipids were quantified as their lithium adducts by comparisons with an internal standard (e.g., lithiated 14:1−14:1 PC) after correction for ^{13}C isotope effects in the positive ion mode as previously described (*24*). Since TAG massively accumulates during differentiation in adipocytes to overwhelm the amount of choline glycerophospholipids

in the cell, it was preferable to separate TAG and choline glycerophospholipids by HPLC as previously described (*26*) prior to ESI-MS analysis. Ethanolamine glycerophospholipids were directly quantified by comparison with an internal standard (e.g., 15:0−15:0 PE) after correction for ^{13}C isotope effects in the negative ion mode as previously described (*24*). Identification of ion peaks was achieved utilizing tandem MS analyses in the precursor ion or neutral loss scanning mode (*25*, *27*). Plasmalogen molecular species were distinguished from alkyl-acyl phospholipid molecular species by treating tissue extracts with acidic vapors prior to mass spectroscopic analyses as described previously (*28*). TAG molecular species were directly quantitated by neutral loss scanning in the positive ion mode as previously described (*25*).

Derivatization of Nonesterified Fatty Acids and Fatty Acids in Individual Lipid Classes. Lipid classes were resolved from the chloroform extract utilizing an Ultrasphere silica HPLC column (4.5 mm × 250 mm, 5 μm, Beckman) as the stationary phase by gradient elution of a mobile phase comprised of hexane, 2-propanol, and 0.005% acetic acid in water at a flow rate of 2 mL/min as described previously (*26*). Nonesterified fatty acids or fatty acids esterified to individual lipid classes were converted to their corresponding methyl esters by incubation of 1−100 μg of lipid in 1 mL of 1 N methanolic HCl at 90 °C for 60 min under nitrogen. After cooling on ice, the mixture was neutralized with Na_2CO_3 and extracted as previously described (*29*). In some cases, monounsaturated fatty acid methyl esters were derivatized with dimethyl disulfide (DMDS) as previously described (*30*). Briefly, to 1−100 μg of fatty acid methyl esters in 0.5 mL of hexane were added dimethyl disulfide (0.5 mL) and I_2 (50 μL of a 60 mg/mL solution in ethyl ether), and the mixture was incubated at 40 °C in an enclosed tube overnight. Iodine was removed by addition of an $Na_2S_2O_3$ solution (5% in distilled water). The reaction mixture was extracted with hexane, dried over $MgSO_4$, filtered, dried under a nitrogen stream, and redissolved in hexane prior to GC−EI-MS analysis (*30*).

Gas Chromatography and Electron Impact Mass Spectrometry of Adipocyte Fatty Acid Methyl Ester. GC−MS was performed on a Thermoquest SSQ 7000 single-stage quadrupole mass spectrometer interfaced with a Varian 3300 gas chromatograph. A fused-silica capillary DB-1 column [12.5 m × 0.2 mm (inside diameter), film thickness of 0.33 μm] from J&W Scientific was employed for separation of fatty acid methyl esters. After injection, the column was held at 120 °C for 1 min prior to increasing the temperature to 270 °C at 10 °C/min and kept at 270 °C for an additional 10 min. For analysis of fatty acid methyl ester DMDS adducts, a DB-17 column [30 m × 0.25 mm (inside diameter), film thickness of 0.25 μm] was used, and the GC oven was maintained at 150 °C for 1 min prior to increasing the temperature to 280 °C at a rate of 30 °C/min and held at 280 °C for an additional 6 min. Helium was used as a carrier gas at a constant pressure of 55 kPa. In all cases, the injector and interline temperatures were maintained at 250 °C. Electron impact (EI) ionization was performed at 70 eV as previously described (*31*).

Indirect Immunofluorescent Microscopy. Six days after differentiation, 3T3-L1 adipocytes were replated at 30−50% of their original density. Adipocytes were fixed for 10 min with 2% formaldehyde in phosphate-buffered saline (PBS). The coverslips were rinsed in PBS and then incubated for 1 h in both PMP70 antiserum (Zymed, San Francisco, CA) diluted 1:1000 in microscopy buffer (1% BSA and 0.1% saponin in PBS) and antibody directed against stearoyl-CoA dehydrogenase at 1 μg/mL (Santa Cruz Biotechnology, Santa Cruz, CA). The coverslips were rinsed in PBS and then incubated for 30 min with Alexa 594 donkey anti-rabbit IgG (Molecular Probes, Eugene, OR) and Alexa 488 donkey anti-goat IgG both diluted 1:1000 in microscopy buffer. To determine if the signal was due to the primary antibody, coverslips were treated as described above with the same concentration of serum or antibody from nonimmunized animals from the appropriate species. Only very faint and diffuse signals were detected in these controls.

α Oxidation of [9,10-^{3}H]Palmitic Acid in 3T3-L1 Cells during Adipocyte Differentiation. 3T3-L1 cells, at selected times during differentiation, were radiolabeled by incubation with 5 μCi of [9,10-^{3}H]palmitic acid (dissolved in EtOH) injected into the incubation medium. After the indicated periods, the medium was removed, the cells were washed with PBS and scraped into 1.5 mL of deionized water, and total lipids were extracted according to the method of Bligh and Dyer with 1% acetic acid in the aqueous layer (*21*). After addition of 100 μg of each internal standard (C16:0, C15:0, and C14:0), the lipids were incubated in 0.4 mL of methanol/0.2 mL of 0.3 M HCl at 60 °C for 20 min to cleave all vinyl ether linkages. The mixture was continuously incubated at 60 °C for an additional 40 min after addition of 1 mL of 1 M KOH. The fatty acids were extracted into hexane (2 × 2 mL) after acidification with 1 M HCl. The extracted fatty acids were dried under a nitrogen stream, redissolved in 0.4 mL of acetone, and oxidized with 1 mL of a 0.1 M $KMnO_4$/0.1 M H_2SO_4 mixture at 60 °C for 20 min. Excess $KMnO_4$ was removed by addition of $Na_2S_2O_3$, and the resulting saturated fatty acids were extracted into hexane (2 × 2 mL) after acidification. Fatty acids were separated by reversed phase HPLC utilizing an octadecyl silica stationary phase (4.6 mm × 250 mm, 5 μm particles) with isocratic elution at 2 min/mL employing a mobile phase comprised of methanol, H_2O, and H_3PO_4 (85:15:0.1, v/v/v). Column eluents were monitored by UV detection at 210 nm, and radioactivity in each saturated fatty acid was quantified by liquid scintillation spectrometry.

[1-^{14}C]Palmitate Oxidation Studies. Assessment of palmitate oxidation was performed as previously described (*32*). Briefly, 3T3-L1 cells were cultured in T-25 flasks to confluence and induced to differentiate as described above. At selected stages of differentiation, [1-^{14}C]palmitate was added to a final concentration of 200 nCi/mL. The flasks were sealed and fitted with a center well comprised of Whatman No. 1 filter paper. At selected time points, the $^{14}CO_2$ liberated from the medium by acidification with 2 mL of 6 M HCl was collected on filter paper previously alkalinized with 250 μL of 2 M NaOH. Released radiolabeled $^{14}CO_2$ was quantified by liquid scintillation counting.

Reverse Transcription and Quantitative Polymerase Chain Reaction (PCR). Total RNA was purified from 3T3-L1 cell pellets by utilizing a RNeasy Mini Kit from Qiagen (Valencia, CA) by following to the manufacturer's instructions. For the preparation of cDNA, 250 pmol of random hexamers was hybridized by incubation for 10 min at 25 °C and

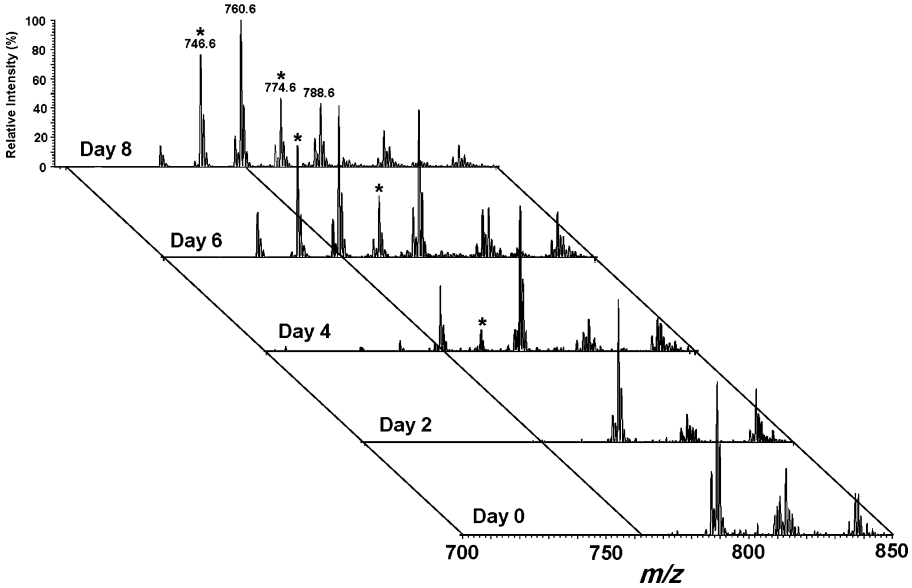

FIGURE 1: Alterations of phosphatidylserine molecular species during hormone-induced differentiation of 3T3-L1 cells. Lipids from 3T3-L1 cells at different stages of differentiation were extracted by a modified Bligh−Dyer technique utilizing 50 mM LiCl in the aqueous layer as described in Experimental Procedures. All samples were diluted in a 1:1 methanol/chloroform mixture prior to direct infusion into the ESI source using a syringe pump at a flow rate of 2 μL/min. Phosphatidylserine molecular species of 3T3-L1 cells at different stages of differentiation were fingerprinted by neutral loss scanning of 87.1 amu in the negative ion mode as described in Experimental Procedures. Mass spectra were normalized to the most intense peak in each individual spectrum. Asterisks denote the molecular species containing odd chain length acyl moieties which are quantified in Table II in the Supporting Information.

extended by incubation for 30 min at 48 °C in the presence of 125 units of reverse transcriptase in 100 μL of PCR buffer [5.5 mM $MgCl_2$, dNTPs (0.5 mM each), and 40 units of RNase inhibitor]. Reverse transcriptase was inactivated by incubation at 95 °C for 5 min. Amplification of each target cDNA was performed with TaqMan PCR reagent kits and quantified by the ABI PRISM 7700 detection system according to the protocol provided by the manufacturer (Applied Biosystems). A traditionally utilized standard gene, GAPDH, was measured and used as an internal standard. Oligonucleotide primer pairs and probes specific for FACO (5′-GGATGGTAGTCCGGAGAACA, 5′-AGTCTGGATCGTTCAGAATCAAG, and 5′-TCTCGATTTCTCGACGGCGCCG) and PAHX (5′-TGAAGAAAATGGGTTTCTCGTCAT, 5′-ACGATCCCTGGTGGTTTCAC, and 5′-ACTCTGCTCGAAAACGTTGA) were employed.

Miscellaneous. Protein concentrations were determined with a BCA protein assay kit (Pierce, Rockford, IL) using bovine serum albumin (BSA) as a standard. All data were normalized to protein content and are presented as the mean ± the standard error of the mean (SEM). Statistically significant differences between mean values were determined with unpaired Student's *t* tests.

RESULTS

Electrospray Ionization Mass Spectrometry of Lipids in Differentiating 3T3-L1 Cells. Mass spectra of serine and inositol glycerophospholipids during hormone-induced differentiation of 3T3-L1 cells demonstrated the time-dependent accumulation of prominent pseudomolecular ion peaks corresponding to odd chain length fatty acids (denoted with asterisks in Figures 1 and 2). Hormone-induced differentiation of 3T3-L1 cells into adipocytes also resulted in a dramatic shift of the aliphatic chains in inositol and serine glycerophospholipids to lower-carbon number molecular species. Both of these features were present in multiple independent preparations (Table 1 and Tables I−V in the Supporting Information). To identify alterations in ethanolamine and choline glycerophospholipids in adipocytes during differentiation, direct ionization of phospholipids from chloroform extracts coupled with neutral loss scanning of their pseudomolecular ions was employed. Mass spectra of choline glycerophospholipids (Figure 3) in differentiating adipocytes demonstrated the robust accumulation of odd chain length molecular species as well as a concurrent shortening of aliphatic chain lengths. Similarly, precursor ion scanning of ethanolamine glycerophospholipids (to clearly visualize each individual molecular species) of day 8 differentiated adipocytes demonstrated accumulation of odd chain length fatty acids and aliphatic chain length shortening (Figure 4 and Table III in the Supporting Information). These results were all confirmed by tandem mass spectrometry employing low-energy collision-induced dissociation. Tandem mass spectrometry of extracts of day 8 adipocytes in the negative ion mode with precursor ion scanning at *m*/*z* 153.0 identified many abundant phosphatidic acid (PA) molecular species which contained odd chain length acyl moieties, including C15:0, C15:1, C17:0, and C17:1 (data not shown). Collectively, these results demonstrate the accumulation of odd chain length molecular species and aliphatic chain length shortening in all major polar lipid classes of the differentiating adipocyte.

Quantitative neutral loss scanning of lipid extracts from differentiated 3T3-L1 adipocytes demonstrated that TAG molecular species were also highly enriched in C15:0, C15:1, C17:0, and C17:1 acyl moieties (Figure 5 and Table V in the Supporting Information). To exclude the possibility that odd chain length fatty acids in adipocytes were the result of C15 and C17 fatty acyl moieties in the culture media, direct analysis of lipids in the nutrient medium was performed. The

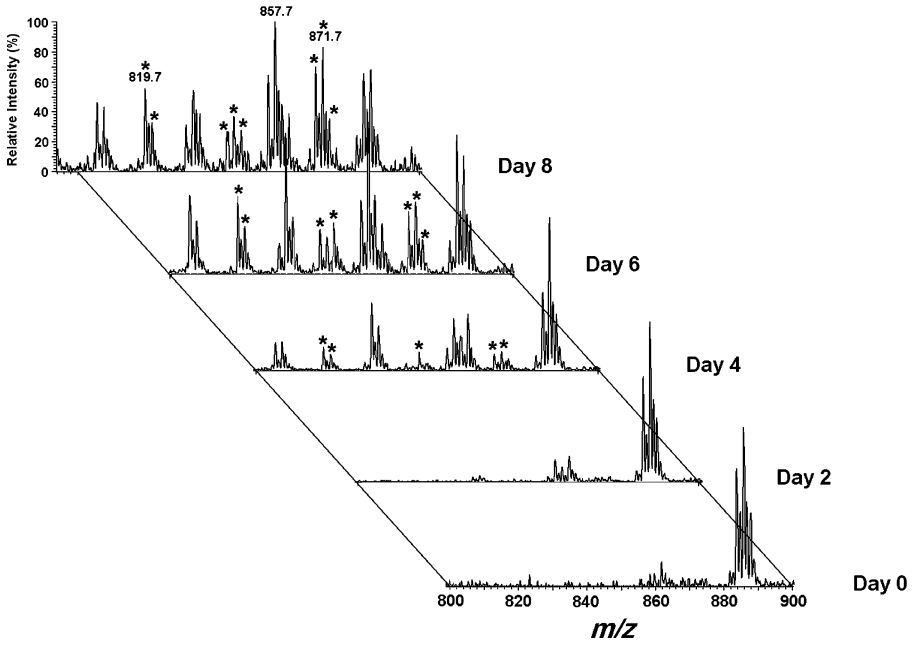

FIGURE 2: Alterations of phosphatidylinositol molecular species during hormone-induced differentiation of 3T3-L1 cells. Lipids from 3T3-L1 cells at different stages of differentiation were extracted by a modified Bligh−Dyer technique utilizing 50 mM LiCl in the aqueous layer as described in Experimental Procedures. All samples were diluted in a 1:1 methanol/chloroform mixture prior to direct infusion into the ESI source using a syringe pump at a flow rate of 2 μL/min. Phosphatidylinositol molecular species were fingerprinted by precursor ion scanning of *m*/*z* 241.2 in the negative ion mode as described in Experimental Procedures. Mass spectra were normalized to the most intense peak in each individual spectrum. Asterisks denote the molecular species containing odd chain length acyl moieties which are quantified in Table I in the Supporting Information.

Table 1: Amounts and Percentages of Total Odd Chain Length Fatty Acyl Moieties in Phospholipids and Triacylglycerol in 3T3-L1 Cells during Hormone-Induced Differentiation[a]

	day 0	day 2	day 4	day 6	day 8
PS	−[c]	−[c]	0.71 (5%)	1.44 (10%)	2.92 (18%)
PI	−[c]	−[c]	1.08 (10%)	2.46 (16%)	3.22 (21%)
PE[b]	3.1 (3%)	8.3 (8%)	39.9 (18%)	44.7 (21%)	60.9 (23%)
PC	−[c]	5.6 (4%)	12.1 (9%)	18.5 (12%)	29.6 (15%)
TAG	−[c]	1.3 (5%)	155 (20%)	524 (27%)	2275 (33%)

[a] Phospholipids and TAG in 3T3-L1 cells during hormone-induced differentiation were extracted and quantified as described in Experimental Procedures. Amounts and percentages of total odd chain length fatty acyl moieties in each phospholipid class and triacylglycerols at different time points of differentiation are presented. The amounts of acyl moieties are presented as nanomoles per milligram of protein. Quantification of individual molecular species of each lipid class is presented in Tables I−V in the Supporting Information. [b] Percentages of each isobaric molecular species were estimated by ESI-MS/MS as described previously (*27*). [c] Less than 1%.

results demonstrated that <1% of the fatty acids in the media was comprised of odd chain length fatty acids. Importantly, both culture media and cytosol contained both oleic acid and palmitoleic acid.

Identification of the Location of Olefinic Linkage in Odd Chain Length Monounsaturated Fatty Acids in Differentiating 3T3-L1 Adipocytes. Identification of the molecular species of TAGs during the differentiation process demonstrated dramatic increases in the amount of TAGs containing unsaturated acyl chains. Remarkably, more than 95% of TAG molecular species contained at least one unsaturated acyl chain (Table V in the Supporting Information). We reasoned that determination of the location of the double bond in the unsaturated odd chain length acyl chains in TAGs could be used to determine if α oxidation and Δ9 desaturation were random or ordered processes in the sequence of reactions leading to fatty acid storage in the TAG compartment of adipocytes. The location of the olefinic linkage in odd chain length fatty acyl moieties would be diagnostic of the order of α oxidation and Δ9 desaturation. For example, if Δ9 desaturation preceded α oxidation in the peroxisomal compartment, then Δ8 unsaturated odd chain length fatty acids would be generated. Similarly, if α oxidation of oleic acid from the medium or cytosol occurred, then Δ8 C17:1 would be produced. Alternatively, if α oxidation of saturated fatty acyl-CoAs obligatorily preceded Δ9 desaturation, then only Δ9 olefins would be present in odd chain length moieties in the TAG pool. If these reactions were random (i.e., there was no obligatory order of α oxidation and Δ9 desaturation), adipocytes would contain both Δ8 and Δ9 unsaturated moieties. To this end, we exploited the propensity of olefinic dimethyl disulfide adducts for α fragmentation during collisional activation of their pseudomolecular ions (*30*). Both C15:1 and C17:1 present in TAG molecular species contained exclusively (>98%) Δ9 desaturated moieties as evidenced by their methylthiol radical-induced fragmentation patterns (Figure 6). These results demonstrate that neither oleic or palmitoleic acid from the medium or cytosol nor SCD desaturated fatty acyl-CoAs can undergo α oxidation since Δ8 olefinic linkages were not observed in either C15:1 or C17:1 species. Thus, α oxidation in the peroxisomal compartment must obligatorily precede Δ9 desaturation. Moreover, once α oxidation has occurred, the processed (i.e., α oxidized) fatty acyl-CoAs can subsequently undergo Δ9 desaturation and thus be metabolically channeled into TAG synthesis. These results demonstrate that one, and perhaps the major, biochemical mechanism underlying the antiadipogenic effects of SCD I knockouts and knockdowns (*33*, *34*) is the metabolic channeling of saturated fatty acids into oxidative pathways since in the absence of Δ9 desaturation

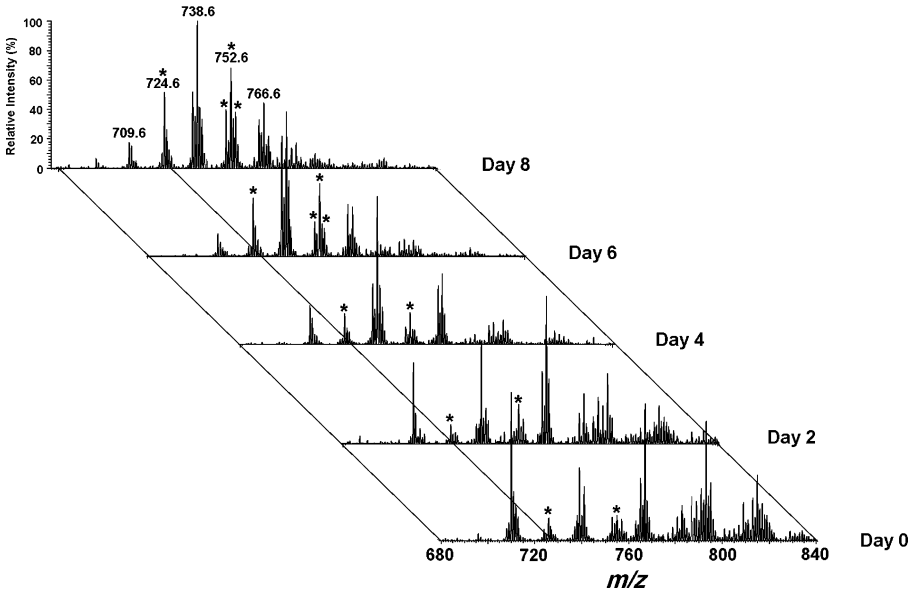

FIGURE 3: Alterations of phosphatidylcholine molecular species from 3T3-L1 cells during hormone-induced differentiation of 3T3-L1 cells. Lipids from 3T3-L1 cells at different stages of differentiation were extracted by a modified Bligh−Dyer technique utilizing 50 mM LiCl in the aqueous layer as described in Experimental Procedures. All samples were diluted in a 1:1 methanol/chloroform mixture, and LiOH (50 nmol/mg of protein) was added just prior to direct infusion into the ESI source using a syringe pump at a flow rate of 2 μL/min. Phosphatidylcholine molecular species were visualized by neutral loss scanning of 183.2 amu in the positive ion mode. All neutral loss mass spectra were displayed after normalization to the most intense peak in the individual spectrum. Asterisks denote the molecular species containing odd chain length acyl moieties which are quantified in Table III in the Supporting Information.

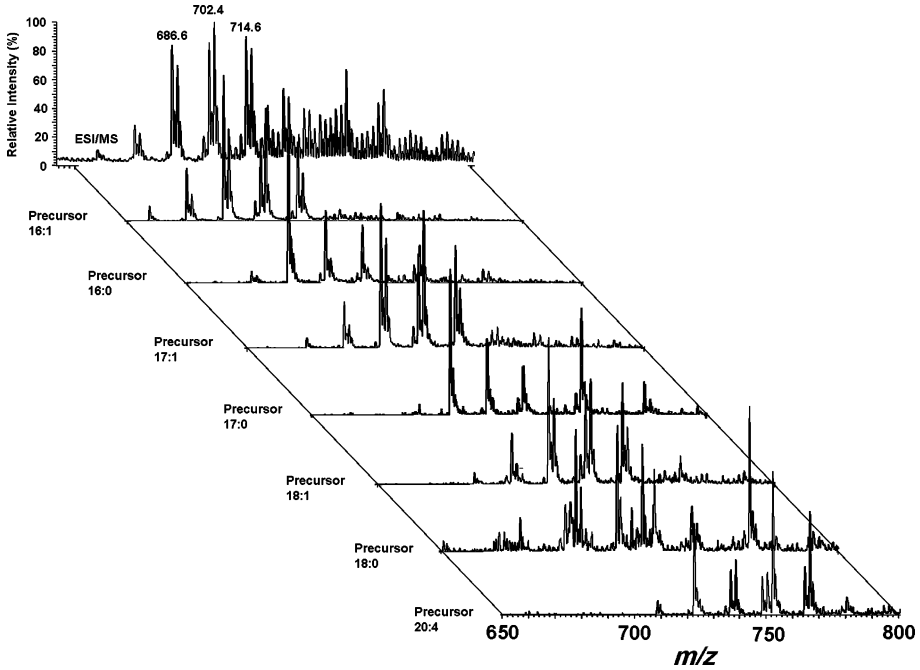

FIGURE 4: Negative ion electrospray ionization mass spectrometry and tandem mass spectrometry of ethanolamine glycerophospholipids from day 8 3T3-L1 cells. Lipids from day 8 3T3-L1 cells were extracted with a modified Bligh−Dyer technique utilizing 50 mM LiCl in the aqueous layer as described in Experimental Procedures. All samples were diluted in a 1:1 methanol/chloroform mixture with addition of LiOH (50 nmol/mg of protein) just prior to their direct infusion into the ESI source using a syringe pump at a flow rate of 2 μL/min. PE molecular species were identified by precursor ion scanning of *m*/*z* 253.2 (16:1), 255.2 (16:0), 267.2 (17:1), 269.2 (17:0), 281.2 (18:1), and 303.2 (20:4) in the negative ion mode. All precursor ion scanning mass spectra were displayed after normalization to the most intense peak in each individual spectrum.

their entry into TAG storage pools is limited (i.e., TAG molecular species contain only diminutive amounts of trisaturated molecular species). Similarly, analysis of odd chain length unsaturated fatty acyl moieties in choline and ethanolamine glycerophospholipids demonstrated the nearly exclusive localization of the double bond at the Δ9 position. Since both culture media and cytosol contained both oleic and palmitoleic acids which possess a double bond exclusively at the Δ9 position (Figure 6E,F), the absence of Δ8 fatty acids in differentiating adipocytes demonstrated that unsaturated fatty acids could not be processed by peroxisomal α oxidation. Thus, once the fatty acids are unsaturated,

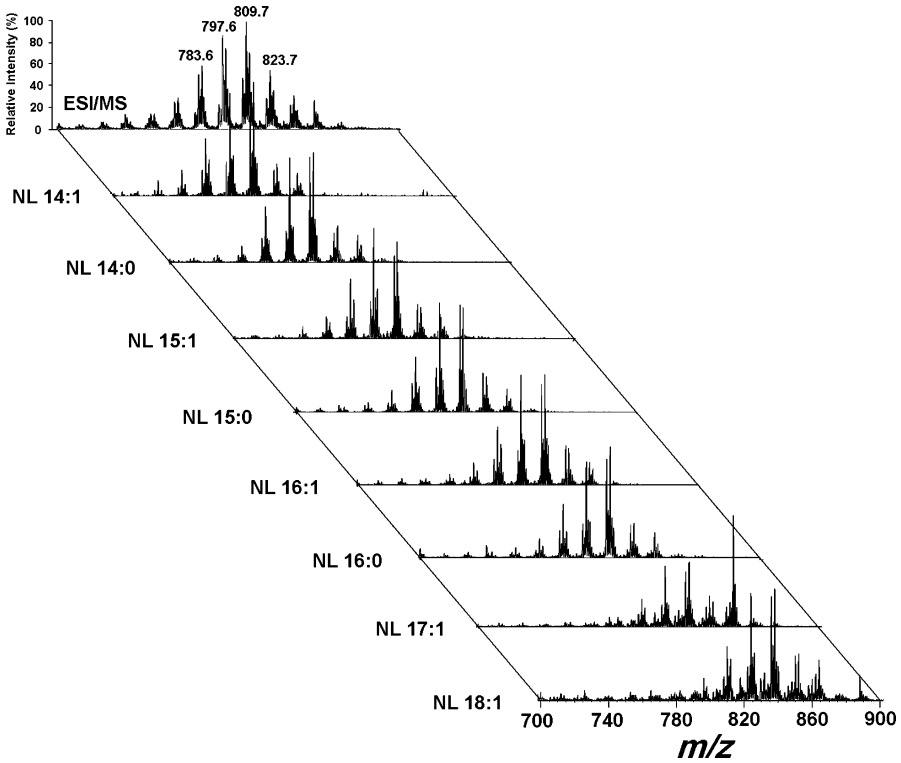

FIGURE 5: Positive ion electrospray ionization mass spectrometry and tandem mass spectra of TAGs from day 8 3T3-L1 cells. Lipids from day 8 3T3-L1 cells were extracted by a modified Bligh−Dyer technique utilizing 50 mM LiCl in the aqueous layer as described in Experimental Procedures. All samples were diluted in a 1:1 methanol/chloroform mixture with addition of LiOH (50 nmol/mg of protein) just prior to direct infusion into the ESI source using a syringe pump at a flow rate of 2 μL/min. Positive ion ESI mass spectra of TAGs in lipid extracts were acquired as described in Experimental Procedures. Positive ion ESI tandem mass spectra by neutral loss scanning of 226.2 (14:1), 228.2 (14:0), 240.2 (15:1), 242.2 (15:0), 254.2 (16:1), 256.2 (16:0), 268.2 (17:1), and 282.2 amu (18:1) were acquired as described in Experimental Procedures. All neutral loss scanning mass spectra were displayed after normalization to the most intense peak in the individual spectrum.

shedding of free energy by α oxidation is not possible and unsaturated fatty acids are channeled toward lipid anabolic pathways.

Recent studies by Hajra and co-workers (*35*) showed that nearly half of TAG synthesis was initiated via the acyl dihydroxyacetone phosphate pathway within the peroxisomal compartment in differentiated adipocytes. The results presented in this study suggest the possibility that peroxisomes could contain a Δ9 desaturase activity since Δ9 desaturation must occur after α oxidation and before the first committed step in TAG synthesis. Neither SCD I nor SCD II has previously been identified in the peroxisomal compartment. However, close inspection of the primary sequence of mouse SCD I revealed a putative type II peroxisomal localization sequence at the N-terminus (**KV**KTVPL**HL**) (*36*−*38*). Further examination of the C-terminus of SCD I identified a dilysine transmembrane ER retention signal (**KK**VS) near the C-terminus (*39*). Thus, mouse SCD I has two putative subcellular localization signals. Prior work has demonstrated a type II PTS consensus sequence is sufficient for peroxisome targeting in many cases (*37*, *38*). However, the large majority of prior studies have assigned SCD I to the ER compartment. Buoyant density gradient centrifugation of hepatic membranes by traditional methods indeed demonstrated that the large majority of SCD I was present in the ER (≈90%). Due to the broad elution of SCD I and the presence of some overlap with peroxisomal markers, the possibility that a small portion of SCD I (≈10%) is present in the peroxisomes could not be ruled out (data not shown). To examine this question in adipocytes, immunohistochemistry of differentiated 3T3-L1 adipocytes was performed. A portion of the SCD I mass appeared to be overlayed with the peroxisomal marker, PMP70 (Figure 7). However, caution must be exercised due to the possibility of emission overlap of opposed or stacked structures. We specifically point out that these results do not describe the subcellular compartment where Δ9 desaturation occurs. The data do demonstrate that no Δ9 desaturated fatty acid can be α oxidized in the peroxisomal compartment, thus increasing the likelihood that Δ9 desaturated fatty acids be recruited into the TAG storage pool.

Production of Radiolabeled C15:0 after Incubation of the Differentiating 3T3-L1 Cells with [9,10-^{3}H]C16:0. To unambiguously demonstrate that the mechanism of production of odd chain length fatty acids in differentiating adipocytes is mediated by α oxidation, initial rate kinetic radiolabeling experiments were performed. Incubation of cells with [9,-10-^{3}H]C16:0 for 0.5, 1, 2, or 5 h resulted in the production of radiolabeled [^{3}H]C15:0. The rate of α oxidation was approximated by calculating the flux of the mass of C16 fatty acids to C15 fatty acids based upon the measured specific activity. For example, cells at day −1, day 4, and day 8 were incubated in radiolabeled C16:0-containing medium (5 μCi in 4 mL of 10% FBS medium). Next, cells were harvested at 0.5, 1, 2, and 5 h, and the radioactivity in the C16 pool was measured. Similarly, the mass of C16:0 NEFA in the adipocytes was measured at these time points. The rate of α oxidation was approximated by calculating the initial rate of conversion of the C16 intracellular

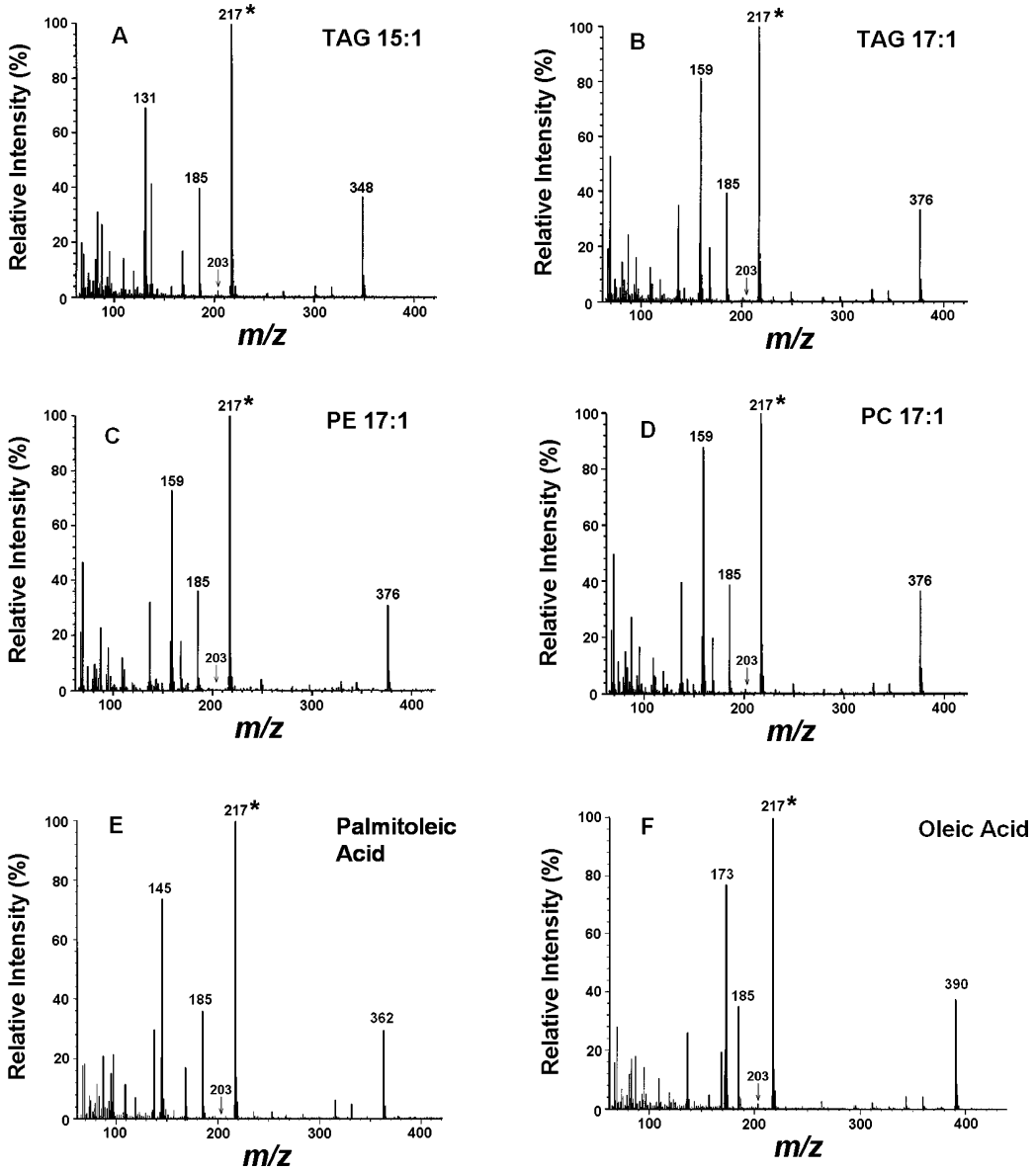

FIGURE 6: Determination of the double bond positions present in odd chain length moieties in TAG, PE, and PC as illustrated by GC−EI-MS of their dimethyl disulfide adducts. Lipids from day 8 3T3-L1 cells were extracted by the method of Bligh and Dyer utilizing 50 mM LiCl in the aqueous phase. Lipid classes were resolved from the chloroform extract utilizing an Ultrasphere silica HPLC column by gradient elution at a flow rate of 2 mL/min as described in Experimental Procedures. The acyl moieties in TAG, PE, and PC were liberated as their methyl esters by acid methanolysis. The resulting monounsaturated fatty acyl methyl esters from each lipid class were converted to their dimethyl disulfide (DMDS) adducts by incubation with dimethyl disulfide and I_2. The resulting DMDS adducts were extracted with hexane and analyzed by GC−MS as described in Experimental Procedures. (A) EI-MS spectra of the C15:1 methyl ester DMDS adduct from TAG. (B) EI-MS spectra of the C17:1 methyl ester DMDS adduct from TAG. (C) EI-MS spectra of the C17:1 methyl ester DMDS adduct from PE. (D) EI-MS spectra of the C17:1 methyl ester DMDS adduct from PC. (E) EI-MS spectra of the palmitoleic acid methyl ester DMDS adduct from the lipid mixture. (F) EI/MS spectra of the oleic acid methyl ester DMDS adduct from the lipid mixture. In all the spectra, asterisks denote *m*/*z* 217, which results from Δ9 fatty methyl ester DMDS adducts. The positions of *m*/*z* 203, which would result from Δ8 fatty methyl ester DMDS adducts but not present in significant amounts, are denoted with arrows.

nonesterified fatty acid mass to the C15 fatty acid mass. Rates of 11, 22, and 45 pmol (mg of protein)$^{-1}$ min^{-1} at day −1, day 4, and day 8 were obtained, respectively (Figure 8A). The measured rate of α oxidation increased 2-fold in day 4 differentiated cells and 4-fold in day 8 differentiated cells in comparison to the rate in resting 3T3-L1 cells (Figure 8A). We point out that this calculation is an estimate since many other factors, including physical or metabolic compartmentalization, are important in the consideration of mass flux. However, we note that by utilizing these basic assumptions, the temporal course of the increase in odd chain length fatty acid mass demonstrated by mass spectrometry parallels the increase in the measured rates of conversion of radiolabeled C16:0 to C15:0.

Fatty Acid Oxidation of [1-^{14}C]Palmitate in Differentiating 3T3-L1 Cells. The rate of total fatty acid oxidation was estimated from measurements of the flux of cells radiolabeled with [1-^{14}C]palmitic acid by calculation of the specific activity of intracellular palmitic acid and the amount of $^{14}CO_2$ production at different times (0.5, 1, 2, or 5 h) after introduction of a label at different times in 3T3-L1 cells after differentiation for −1, 4, and 8 days. From the measurements of radiolabeled C16 NEFA and C16 NEFA mass, the specific activity of C16 fatty acid could be calculated and the

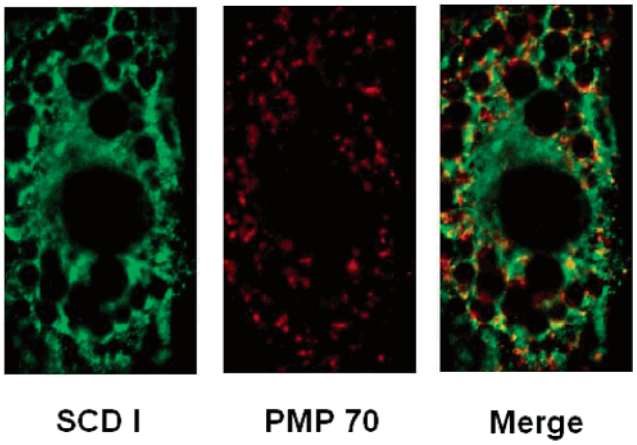

FIGURE 7: Immunohistochemistry of SCD I in differentiated adipocytes. Six days after differentiation, 3T3-L1 adipocytes were replated at 30−50% of their original density. Adipocytes were fixed for 10 min with 2% formaldehyde in phosphate-buffered saline (PBS). The coverslips were rinsed in PBS and then incubated for 1 h in both PMP70 antiserum (diluted 1:500 in microscopy buffer) and anti-stearoyl-CoA dehydrogenase (1 μg/mL). The coverslips were rinsed in PBS and then incubated for 30 min with 594 donkey anti-rabbit IgG and 488 donkey anti-goat IgG both diluted 1:1000 in microscopy buffer: SCD I (left), PMP 70 (middle), and merged (right).

appearance of $^{14}CO_2$ was used to approximate the overall rate of fatty acid oxidation (both α and β oxidation) as described above. Again, we point out that these results represent a first-order approximation which does not take into account issues related to compartmentalization (either physical or metabolic). Utilizing these approximations, the results demonstrated that fatty acids are oxidized at similar rates in day −1 and day 4 cells but that by day 8 the adipocyte has dramatically increased its oxidative rate (Figure 8B). Remarkably, the increase in its rate of α oxidation accounts for the main increase in the oxidative rate of differentiated 3T3-L1 cells.

Quantitative PCR Analysis of PAHX and FACO RNA Levels. Since α hydroxylation, which presumably is initiated by PAHX, is the first committed step, and one of the rate-determining steps, in odd chain length FA production (*15*), PAHX mRNA levels were examined after differentiation was induced. As expected, the PAHX mRNA level increased 4-fold during differentiation (Figure 9A). This result supports the data that the level of straight chain fatty acid α oxidation increases during adipocyte differentiation. Moreover, the mRNA level of FACO, whose protein product catalyzes the rate-determining step of peroxisomal fatty acid β oxidation, also dramatically increased during differentiation (Figure 9B). The proliferation of peroxisomes in conjunction with the entry of their metabolic products into lipid storage pools supports the role of peroxisomes in modulating lipid metabolism during adipocyte differentiation (*40*, *41*).

DISCUSSION

The synthesis and catabolism of fatty acids in mammalian cells have been extensively studied over the past 50 years. This study utilizes recent advances in lipidomics (*42*) to demonstrate dramatic changes in cellular lipid metabolism that accompany 3T3-L1 cell differentiation into adipocytes after hormone-induced differentiation. Through the detailed account of time-dependent alterations of the individual

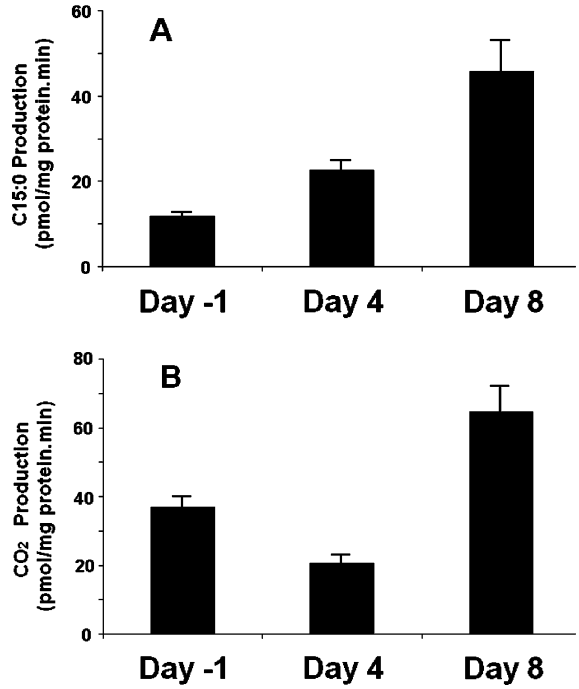

FIGURE 8: Fatty acid oxidation of exogenously administered fatty acids in 3T3-L1 cells during differentiation. (A) 3T3-L1 cells at selected times during differentiation were radiolabeled by incubation with 5 μCi of [9,10-^{3}H]palmitic acid by ethanolic injection into the incubation medium. After 0.5, 1, 2, and 5 h, the medium was removed, the cells were washed with PBS and scraped into 1.5 mL of deionized water, and total lipids were extracted according to the method of Bligh and Dyer with 1% acetic acid in the aqueous layer. The initial rates of conversion of radiolabeled C16:0 into C15:0 fatty acids were quantified as described in Experimental Procedures. Unlabeled nonesterified fatty acids were purified and their concentrations determined as described in Experimental Procedures. The α oxidation rate was approximated by estimating the initial flux of C16:0 to C15:0 mass as described in Experimental Procedures. (B) 3T3-L1 cells were cultured in T-25 flasks to confluence and induced to differentiate. At selected differentiation stages, [1-^{14}C]palmitate was added to a final concentration of 200 nCi/mL. The flasks were sealed and fitted with a center well comprised of Whatman No. 1 filter paper. After 0.5, 1, 2, and 5 h, the $^{14}CO_2$ liberated from the medium by acidification with 2 mL of 6 M HCl was collected on the filter paper previously alkalinized with 250 μL of 2 M NaOH. Released radiolabeled $^{14}CO_2$ was quantified by liquid scintillation counting. The fatty acid oxidation rate was approximated by calculating the initial rate of production of $^{14}CO_2$ as described in Experimental Procedures.

chemical constituents present in adipocyte cellular membranes and TAG storage pools, new insights into the cellular processing of fatty acids in mammalian cells have been gleaned. The importance of fatty acid α oxidation and the obligatory sequential ordered processing of α oxidation of fatty acids prior to their Δ9 desaturation and subsequent incorporation into TAG molecular species in this murine cell line have been determined.

Prior work has demonstrated the importance of SCD I in both diet and leptin-mediated obesity (*33*, *34*). For example, SCD I null mice do not become obese in response to high-fat diets. Similarly, genetic crosses of SCD I null mice with leptin-deficient mice demonstrate that SCD I deficiency protects against the obesity that is manifested in leptin-deficient mice. Several clues to the chemical mechanisms underlying these recent important physiologic and genetic observations can be gleaned from careful analysis of the individual molecular species changes that occur during the

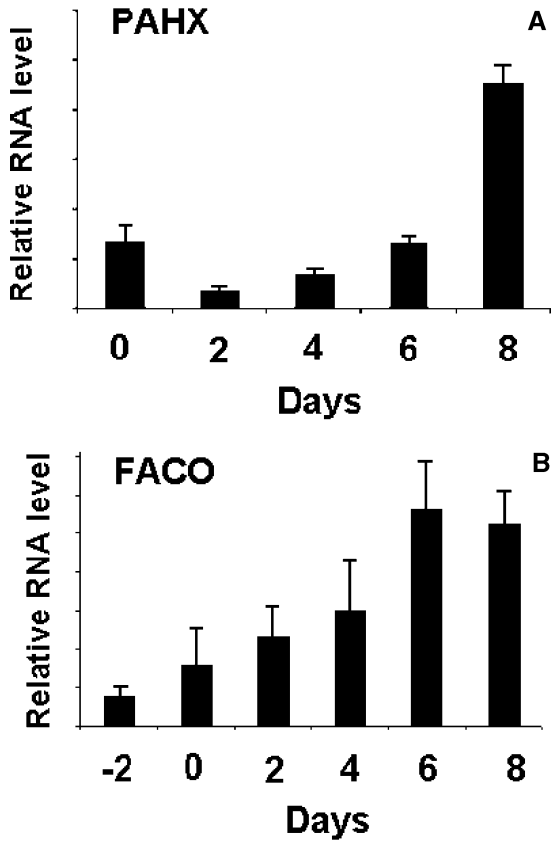

FIGURE 9: Messenger RNA levels of FACO and PAHX in 3T3-L1 cells during differentiation. 3T3-L1 cells were cultured and induced to differentiate as described in Experimental Procedures. At indicated differentiation stages, total RNA was prepared as described in Experimental Procedures. Quantitative PCR was performed with TaqMan PCR reagent kits in the ABI PRISM 7700 detection system utilizing GAPDH as the internal standard. A representative result of three independent experiments is shown.

adipocyte differentiation process. First, molecular species analysis of TAGs in differentiating adipocytes demonstrates that the overwhelming majority (>95%) of TAG molecular species contain unsaturated fatty acids. Since the aliphatic chains entering the TAG pool are largely derived from saturated fatty acids in the growth medium (palmitate and stearate are the most abundant fatty acids in the growth medium) and saturated fatty acids derived from *de novo* synthetic pathways, it is clear that fatty acid desaturation is an important process in providing the specific building blocks (desaturated fatty acids) used in TAG synthesis. Second, these results show that saturated fatty acids can be rapidly α oxidized after differentiation (but not in undifferentiated cells) and that the levels of mRNAs encoding enzymes involved in peroxisomal fatty acid oxidation are increased. Moreover, in differentiated adipocytes, the rate of α oxidation is robust and by first-order approximation is likely at least as robust as the rate of β oxidation. We specifically point out that the effects of compartmentalization (both physical and metabolic) make these interpretations only approximate. Nonetheless, it seems apparent both in the mass increase of odd chain length fatty acids and in the direct measurements of C16 to C15 conversion that substantial α oxidation of unbranched fatty acids is occurring in the differentiating adipocyte. Third, these results also demonstrate that after α oxidation in the peroxisomes, odd chain length fatty acids can subsequently be desaturated by Δ9 desaturase. Of note is the demonstration of a putative type 2 peroxisomal localization sequence in the primary sequence of mouse SCD I. This sequence motif has previously been shown to be sufficient for peroxisomal membrane integration by others (*37*). Both buoyant density gradient centrifugation data and immunohistochemistry were consistent with the notion that a small portion of SCD I resides in the peroxisomal compartment. The desaturase activity of SCD I requires cytochrome b_5 and an electron donor. Previous studies have utilized several different techniques to demonstrate that a portion of cytochrome b_5 is associated with the peroxisomal compartment (*43*, *44*). Moreover, a very recent publication demonstrated the presence of cytochrome b_5 and cytochrome b_5 reductase in highly purified hepatic peroxisomes (*45*). We specifically point out that these results do not exclude the possibility that after α oxidation in the peroxisomal compartment subsequent Δ9 desaturation can occur in the ER if the odd chain length peroxisomal acyl-CoA is hydrolyzed, transported to the ER (by either directed or passive diffusion), and subsequently Δ9 desaturated. Wherever the specific anatomic compartment in which Δ9 desaturation occurs is located, the results collectively demonstrate the functional sequential ordered processes of α oxidation prior to Δ9 desaturation in differentiating adipocytes. In large part, this is due to the inability of unsaturated fatty acids to serve as substrates for α oxidation. Fourth, since odd chain length fatty acids containing Δ9 unsaturated centers are abundant TAG molecular species in differentiated adipocytes, these results underscore the quantitative importance of sequential α oxidation and Δ9 desaturation in generating the aliphatic constituents used to build TAG molecular species. Finally, the proximity of TAG lipid droplets to the peroxisomal compartment in conjunction with the mass spectrometric data raises the intriguing possibility that multiple functionally important interactions exist between peroxisomes and TAG droplets (*40*, *41*). Collectively, these results demonstrate the obligatory ordering of α oxidation and Δ9 desaturation and the importance of peroxisomal lipid metabolism in generating the lipid molecular species present in the lipidome of differentiating adipocytes.

In resting 3T3-L1 cells, only diminutive amounts of odd chain length fatty acids are present and the molecular species distribution in each class of lipids is similar to that found in many other cell types (e.g., inositol glycerophospholipids have predominantly 18:0−20:4 molecular species). However, within days of hormone-induced differentiation, the level of odd chain length fatty acids began to increase in multiple different lipid classes. Prior work has demonstrated that the peroxisomal enzyme phytanoyl-CoA α hydroxylase can utilize unbranched fatty acids as substrates (*15*), and our study demonstrates that the level of PAHX mRNA is increased 4-fold during adipocyte differentiation. Since α hydroxylation is the first committed step, and one of the rate-determining steps, in odd chain length FA production (*13*, *15*), the observed increase in the level of α oxidation is presumably mediated by a transcription-mediated increase in the amount of phytanoyl-CoA α hydroxylase mRNA, followed by its translation and PAHX-catalyzed α oxidation in the peroxisomal compartment. Post-translational alterations may also contribute to the observed increase in the level of α oxidation. Early studies have failed to demonstrate the presence of α hydroxylation catalyzed by this enzyme

utilizing long chain unbranched fatty acids as substrates (*14*). However, the recent demonstration of the importance of substrate presentation mediated by sterol carrier protein 2 (and perhaps additional proteins as well in peroxisomes) makes it likely that α oxidation in the peroxisomal compartment is catalyzed by phytanoyl-CoA α hydroxylase utilizing SCP 2 or other proteins to facilitate substrate presentation (*15*). Recent studies suggesting the importance of α oxidation emerged when multiple enzymes involved in the peroxisomal α-hydroxyl fatty acid oxidation have been cloned from both rat and human genomes, leading to the expression of protein products with high activity utilizing α-hydroxy unbranched long chain fatty acids (e.g., α-hydroxylpalmitic acid) as substrates (*46*−*48*).

Since α oxidation utilizes O_2 as a direct electron acceptor, this reaction does not produce any reducing equivalents which can be utilized for ATP synthesis. Thus, α oxidation in the peroxisomal compartment is constitutively uncoupled and serves as a *de facto* mechanism for shedding the Gibbs free energy inherent in the C−C bond of fatty acids (i.e., thermogenesis). Moreover, α oxidation produces CO_2 at the expense of acetyl-CoA production and thus does not participate in the efficient conversion of fatty acid into chemical fuel for cellular utilization. Thus, these results indicate a prominent role for fatty acid α oxidation as an important metabolic determinant of the lipid content in the differentiating adipocyte. Collectively, they underscore the role of fatty acid α oxidation in the peroxisomal compartment as a proximal mechanism which modulates fatty acid metabolic fate and energy storage in the differentiating adipocyte.

ACKNOWLEDGMENT

We thank Dr. Nathan E. Wolins for help with the immunofluorescent microscopy.

SUPPORTING INFORMATION AVAILABLE

Quantification of individual molecular species of PI, PS, PE, PC, and TAG in 3T3-L1 cells during hormone-induced differentiation into adipocytes. This material is available free of charge via the Internet at http://pubs.acs.org.

REFERENCES

1. Friedman, J. M. (2000) Obesity in the new millennium, *Nature 404*, 632−634.
2. Kopelman, P. G. (2000) Obesity as a medical problem, *Nature 404*, 635−643.
3. Gregoire, F. M., Smas, C. M., and Sul, H. S. (1998) Understanding adipocyte differentiation, *Physiol. Rev. 78*, 783−809.
4. Pi-Sunyer, X. (2003) A clinical view of the obesity problem, *Science 299*, 859−860.
5. Spiegelman, B. M., and Flier, J. S. (2001) Obesity and the regulation of energy balance, *Cell 104*, 531−543.
6. Lowell, B. B., and Spiegelman, B. M. (2000) Towards a molecular understanding of adaptive thermogenesis, *Nature 404*, 652−660.
7. Green, H., and Kehinde, O. (1975) An established preadipose cell line and its differentiation in culture. II. Factors affecting the adipose conversion, *Cell 5*, 19−27.
8. Green, H., and Kehinde, O. (1976) Spontaneous heritable changes leading to increased adipose conversion in 3T3 cells, *Cell 7*, 105−113.
9. Reginato, M. J., Krakow, S. L., Bailey, S. T., and Lazar, M. A. (1998) Prostaglandins promote and block adipogenesis through opposing effects on peroxisome proliferator-activated receptor g, *J. Biol. Chem. 273*, 1855−1858.
10. Alexander, M., Curtis, G., Avruch, J., and Goodman, H. M. (1985) Insulin regulation of protein biosynthesis in differentiated 3T3 adipocytes. Regulation of glyceraldehyde-3-phosphate dehydrogenase, *J. Biol. Chem. 260*, 11978−11985.
11. Green, H., and Kehinde, O. (1979) Formation of normally differentiated subcutaneous fat pads by an established preadipose cell line, *J. Cell. Physiol. 101*, 169−171.
12. Wanders, R. J., Jansen, G. A., and Lloyd, M. D. (2003) Phytanic acid α-oxidation, new insights into an old problem: a review, *Biochim. Biophys. Acta 1631*, 119−135.
13. Wanders, R. J., Vreken, P., Ferdinandusse, S., Jansen, G. A., Waterham, H. R., van Roermund, C. W., and Van Grunsven, E. G. (2001) Peroxisomal fatty acid α- and *β*-oxidation in humans: enzymology, peroxisomal metabolite transporters and peroxisomal diseases, *Biochem. Soc. Trans. 29*, 250−267.
14. Croes, K., Foulon, V., Casteels, M., Van Veldhoven, P. P., and Mannaerts, G. P. (2000) Phytanoyl-CoA hydroxylase: recognition of 3-methyl-branched acyl-coAs and requirement for GTP or ATP and Mg^{2+} in addition to its known hydroxylation cofactors, *J. Lipid Res. 41*, 629−636.
15. Mukherji, M., Kershaw, N. J., Schofield, C. J., Wierzbicki, A. S., and Lloyd, M. D. (2002) Utilization of sterol carrier protein-2 by phytanoyl-CoA 2-hydroxylase in the peroxisomal α oxidation of phytanic acid, *Chem. Biol. 9*, 597−605.
16. Jansen, G. A., van den Brink, D. M., Ofman, R., Draghici, O., Dacremont, G., and Wanders, R. J. (2001) Identification of pristanal dehydrogenase activity in peroxisomes: conclusive evidence that the complete phytanic acid α-oxidation pathway is localized in peroxisomes, *Biochem. Biophys. Res. Commun. 283*, 674−679.
17. Jansen, G. A., Ofman, R., Denis, S., Ferdinandusse, S., Hogenhout, E. M., Jakobs, C., and Wanders, R. J. (1999) Phytanoyl-CoA hydroxylase from rat liver. Protein purification and cDNA cloning with implications for the subcellular localization of phytanic acid α-oxidation, *J. Lipid Res. 40*, 2244−2254.
18. Verhoeven, N. M., and Jakobs, C. (2001) Human metabolism of phytanic acid and pristanic acid, *Prog. Lipid Res. 40*, 453−466.
19. Mihalik, S. J., Morrell, J. C., Kim, D., Sacksteder, K. A., Watkins, P. A., and Gould, S. J. (1997) Identification of PAHX, a Refsum disease gene, *Nat. Genet. 17*, 185−189.
20. Frost, S. C., and Lane, M. D. (1985) Evidence for the involvement of vicinal sulfhydryl groups in insulin-activated hexose transport by 3T3-L1 adipocytes, *J. Biol. Chem. 260*, 2646−2652.
21. Bligh, E. G., and Dyer, W. J. (1959) A rapid method of total lipide extraction and purification, *Can. J. Biochem. Physiol. 37*, 911−917.
22. Han, X., and Gross, R. W. (1994) Electrospray ionization mass spectroscopic analysis of human erythrocyte plasma membrane phospholipids, *Proc. Natl. Acad. Sci. U.S.A. 91*, 10635−10639.
23. Han, X., Gubitosi-Klug, R. A., Collins, B. J., and Gross, R. W. (1996) Alterations in individual molecular species of human platelet phospholipids during thrombin stimulation: electrospray ionization mass spectrometry-facilitated identification of the boundary conditions for the magnitude and selectivity of thrombin-induced platelet phospholipid hydrolysis, *Biochemistry 35*, 5822−5832.
24. Han, X., Abendschein, D. R., Kelley, J. G., and Gross, R. W. (2000) Diabetes-induced changes in specific lipid molecular species in rat myocardium, *Biochem. J. 352*, 79−89.
25. Han, X., and Gross, R. W. (2001) Quantitative analysis and molecular species fingerprinting of triacylglyceride molecular species directly from lipid extracts of biological samples by electrospray ionization tandem mass spectrometry, *Anal. Biochem. 295*, 88−100.
26. Ford, D. A., Han, X., Horner, C. C., and Gross, R. W. (1996) Accumulation of Unsaturated Acylcarnitine Molecular Species During Acute Myocardial Ischemia: Metabolic Compartmentalization of Products of Fatty Acyl Chain Elongation in the Acylcarnitine Pool, *Biochemistry 35*, 7903−7909.
27. Han, X., and Gross, R. W. (1995) Structural determination of picomole amounts of phospholipids via electrospray ionization tandem mass spectrometry, *J. Am. Soc. Mass Spectrom. 6*, 1202−1210.
28. Ford, D. A., Rosenbloom, K. B., and Gross, R. W. (1992) The primary determinant of rabbit myocardial ethanolamine phosphotransferase substrate selectivity is the covalent nature of the sn-1 aliphatic group of diradyl glycerol acceptors, *J. Biol. Chem. 267*, 11222−11228.

29. Gross, R. W. (1984) High plasmalogen and arachidonic acid content of canine myocardial sarcolemma: a fast atom bombardment mass spectroscopic and gas chromatography−mass spectroscopic characterization, *Biochemistry 23*, 158−165.
30. Buser, H. R., Arn, H., Guerin, P., and Rauscher, S. (1983) Determination of double bond position in mono-unsaturated acetates by mass spectrometry of dimethyl disulfide adducts, *Anal. Chem. 55*, 818−822.
31. Ryhage, R., and Stenhagen, E. (1960) Mass spectrometry in lipid research, *J. Lipid Res. 1*, 361−390.
32. Gulick, T., Cresci, S., Caira, T., Moore, D. D., and Kelly, D. P. (1994) The peroxisome proliferator-activated receptor regulates mitochondrial fatty acid oxidative enzyme gene expression, *Proc. Natl. Acad. Sci. U.S.A. 91*, 11012−11016.
33. Cohen, P., Miyazaki, M., Socci, N. D., Hagge-Greenberg, A., Liedtke, W., Soukas, A. A., Sharma, R., Hudgins, L. C., Ntambi, J. M., and Friedman, J. M. (2002) Role for stearoyl-CoA desaturase-1 in leptin-mediated weight loss, *Science 297*, 240−243.
34. Ntambi, J. M., Miyazaki, M., Stoehr, J. P., Lan, H., Kendziorski, C. M., Yandell, B. S., Song, Y., Cohen, P., Friedman, J. M., and Attie, A. D. (2002) Loss of stearoyl-CoA desaturase-1 function protects mice against adiposity, *Proc. Natl. Acad. Sci. U.S.A. 99*, 11482−11486.
35. Hajra, A. K., Larkins, L. K., Das, A. K., Hemati, N., Erickson, R. L., and MacDougald, O. A. (2000) Induction of the peroxisomal glycerolipid-synthesizing enzymes during differentiation of 3T3-L1 adipocytes. Role in triacylglycerol synthesis, *J. Biol. Chem. 275*, 9441−9446.
36. Ntambi, J. M., Buhrow, S. A., Kaestner, K. H., Christy, R. J., Sibley, E., Kelly, T. J., Jr., and Lane, M. D. (1988) Differentiation-induced gene expression in 3T3-L1 preadipocytes. Characterization of a differentially expressed gene encoding stearoyl-CoA desaturase, *J. Biol. Chem. 263*, 17291−17300.
37. Rachubinski, R. A., and Subramani, S. (1995) How proteins penetrate peroxisomes, *Cell 83*, 525−528.
38. Subramani, S. (1996) Protein translocation into peroxisomes, *J. Biol. Chem. 271*, 32483−32486.
39. Teasdale, R. D., and Jackson, M. R. (1996) Signal-mediated sorting of membrane proteins between the endoplasmic reticulum and the golgi apparatus, *Annu. Rev. Cell Dev. Biol. 12*, 27−54.
40. Blanchette-Mackie, E. J., Dwyer, N. K., Barber, T., Coxey, R. A., Takeda, T., Rondinone, C. M., Theodorakis, J. L., Greenberg, A. S., and Londos, C. (1995) Perilipin is located on the surface layer of intracellular lipid droplets in adipocytes, *J. Lipid Res. 36*, 1211−1226.
41. Novikoff, A. B., Novikoff, P. M., Rosen, O. M., and Rubin, C. S. (1980) Organelle relationships in cultured 3T3-L1 preadipocytes, *J. Cell Biol. 87*, 180−196.
42. Han, X., and Gross, R. W. (2003) Global analyses of cellular lipidomes directly from crude extracts of biological samples by ESI mass spectrometry: A bridge to lipidomics, *J. Lipid Res. 44*, 1071−1079.
43. Fowler, S., Remacle, J., Trouet, A., Beaufay, H., Berthet, J., Wibo, M., and Hauser, P. (1976) Analytical study of microsomes and isolated subcellular membranes from rat liver. V. Immunological localization of cytochrome b5 by electron microscopy: methodology and application to various subcellular fractions, *J. Cell Biol. 71*, 535−550.
44. Appelkvist, E. L., Brunk, U., and Dallner, G. (1981) Isolation of peroxisomes from rat liver using sucrose and Percoll gradients, *J. Biochem. Biophys. Methods 5*, 203−217.
45. Kikuchi, M., Hatano, N., Yokota, S., Shimozawa, N., Imanaka, T., and Taniguchi, H. (2004) Proteomic Analysis of Rat Liver Peroxisome: Presence of Peroxisome-Specific Isozyme of Lon Protease, *J. Biol. Chem. 279*, 421−428.
46. Belmouden, A., Le, K. H., Lederer, F., and Garchon, H. J. (1993) Molecular cloning and nucleotide sequence of cDNA encoding rat kidney long-chain L-2-hydroxy acid oxidase. Expression of the catalytically active recombinant protein as a chimaera, *Eur. J. Biochem. 214*, 17−25.
47. Diep Le, K. H., and Lederer, F. (1991) Amino acid sequence of long chain α-hydroxy acid oxidase from rat kidney, a member of the family of FMN-dependent α-hydroxy acid-oxidizing enzymes, *J. Biol. Chem. 266*, 20877−20881.
48. Jones, J. M., Morrell, J. C., and Gould, S. J. (2000) Identification and characterization of HAOX1, HAOX2, and HAOX3, three human peroxisomal 2-hydroxy acid oxidases, *J. Biol. Chem. 275*, 12590−12597.

BI035867Z